Vortex shedding flowmeters for high velocity liquids*

J. D. Siegwarth
Chemical Engineering Science Division, National Institute of Standards and Technology†, Boulder, CO, USA

The applicability of vortex shedding flowmeters to measurement in the space shuttle main engine (SSME) ducts is reported here. The liquid oxygen (LOX) flows in the engine ducts exceed by as much as a factor of 10 the maximum flow velocities for which commercially available meters are designed. The largest Reynolds number is about 3×10^7. Tests results show that the vortex shedding flowmeters can measure flow in the SSME ducts and do so without any upstream flow conditioning. The meter measuring element for meter bores up to 59 mm can be introduced through an opposed pair of standard SSME duct instrument ports.

Keywords: flow measurement; vortex shedding; liquid oxygen

Introduction

Flow measurement in the fuel and oxidizer ducts of liquid fueled rocket engines is desired for health monitoring and control. The flow-measuring environment in the ducts of the SSME is extreme. Pressure, temperature, flow velocity, and vibration levels are well beyond those generally encountered in terrestrial flow metering applications. The ducts are short and have so many bends that straight sections, where flowmeters can be located, are short. Venturi and turbine meters have been used for duct flow measurements. In this work, sponsored by the National Aeronautic and Space Administration (NASA), the application of vortex shedding (VS) flowmeters to SSME duct measurements is being examined. This paper reports the work on VS meter designs to measure flow of liquid oxygen.

The high flow velocities and the absence of straight sections for the meters appeared to offer the most serious impediments to the use of VS meters. The maximum LOX flow velocity in the ducts of the SSME is an estimated 56 m/s (185 ft/s). The corresponding Reynolds number (Re) is about 3×10^7. This velocity is nearly 10 times greater than the maximum for which commercial liquid vortex meters are designed. The high flows would result in a large pressure drop across a commercial meter since the pressure loss is proportional to square of the flow velocity. A common recommendation by manufacturers for the installation of VS meters is 20 diameters of straight pipe preceding the meter and 5 diameters succeeding. The ducts of the SSME seldom have straight sections exceeding 10 diameters in length in which to install meters. Additional limitations were imposed on the meter design by the desire that the meter be inserted into the smaller ducts through either one or a pair of the 11.2 mm (0.44 inch) diameter standard instrument ports used on the ducts.

The testing was first directed toward demonstrating that the VS meter could measure flow in straight ducts at the high flows without excessive pressure loss before doing tests in actual SSME ducts. It was assumed that water could be used as a substitute fluid for LOX for much of the testing. Cryogenic testing of candidate meters would then be carried out on the test stand at NASA Marshall Space Flight Center.

The object of this work has been to produce meter designs that will work in the SSME ducts at specified locations. Defining and detailing the design parameters has been pursued only to the point that a particular design measures flow satisfactorily. Earlier portions of this work have been reported elsewhere.[1–3]

The vortex shedding flowmeter

Only a brief description of the vortex shedding flowmeter will be given here since many descriptions have already been published.[4–7]

A body of uniform cross section with its axis perpendicular to a uniform flow field will alternately shed vortices from the sides when the flow attains a sufficiently high Reynolds number.[8] Over a wide flow range the shedding frequency f can be proportional to the flow velocity V. This relationship is expressed by the Strouhal equation $f = SV/w$, where w is the width of the body transverse to the flow and S is the Strouhal number which is nominally a constant over a wide range of flows. This equation holds even when the body, or vane, is enclosed in a pipe with the body axis on a pipe diameter.

In a pipe, V at the vane becomes a function of w in such a way that if f/V is plotted as a function of w/D where D is the pipe diameter, a minimum is found in the region of $w/D = 0.25$ to 0.4 depending on the cross-sectional shape of the vane. Other workers have shown that the stability and periodicity of vortex shedding is best when w/D is in the vicinity of this minimum.[9] The meter calibration is also the least sensitive to manufacturing variations and wear when a value of w/D near the minimum is chosen.[9]

The strength and regularity of the shedding and the constancy of S with flow rate are all affected by the cross-sectional-shape of the vane. An examination of some of the cross-sectional shapes available in commercial meters, rectangular, triangular, trapezoidal, and T shapes, suggested that one "ideal" shape may not exist.[4–7] One feature common to many vanes is that the upstream surface consists of a flat face with sharp corners

* Contribution of National Institute of Standards and Technology. Not subject to copyright.
† Formerly National Bureau of Standards.
Address reprint requests to Dr. Siegwarth at the Chemical Engineering Science Division, National Institute of Standards and Technology, 325 Broadway, Boulder, CO 80303, USA.
Received 27 May 1987; accepted 20 January 1989

set perpendicular to the flow. The face width is usually the widest part of the vane. Even this flat face is not universal.

Other authors have presented studies of the effects of vane shapes for flowmeters operating at conventional flows.[9-12] It was not obvious, however, that their results would apply to the higher flow velocities in the SSME ducts.

Experimental methods

Existing water flow test facilities were inadequate to test meters to high flow because of the high inlet pressure needed to achieve these high flows. The simple test facility shown in Figure 1 was constructed to do the testing. The initial test section had a $1\frac{1}{2}$-inch nominal (41 mm actual) bore in which flow velocities of about 56 m/s (185 ft/s) were desired. Rather than using the large motor and pump necessary to achieve the required flows, the test facility was connected to the penstock of a Pelton wheel at a small power plant. The available head was 556 m (1828 ft or 790 psi) and the available flow was in excess of 1 m^3/s. Later, when lower maximum flow velocities were sufficient, the test facility of Figure 1 was moved to another location on the same penstock where 395 m (1300 ft or 570 psi) maximum head was available.

The average flow velocity in the test section was obtained from a calibrated 4-inch vortex shedding flowmeter upstream of the test section. This meter had been calibrated for earlier flow work over the lower half of the range used. A small slope amounting to a 0.7% change over the range of 0 to 10 m/s flow velocity was ignored and an averaged calibration constant was used. The $1\frac{1}{2}$-inch test section size used for the majority of the early tests was chosen to limit pressure loss in the upstream piping and still be large enough to start the testing with a commercially designed meter.

No pressure control at the flowmeter was available in this simple flow test apparatus. As the flow increased the pressure at the test meter declined. More than 1.4 MPa (200 psi) head was converted to kinetic energy in attaining the maximum flow velocity. The available head for the tests also varied during the summer depending on the draw to a water treatment plant taking water from the same penstock. The available head varied especially after the test facility was moved to the site with 395 m head. Pressures at the meter were measured initially to establish the pressure drop ΔP across the meter. A pair of taps, one three diameters upstream of the meter and the other three diameters downstream, were used to measure the pressure loss and the pressures in the duct. The upper flow limit of the meter was the only parameter that changed with pressure. Since freezing of the pressure lines could occur at the test site through much of the year, pressure measurements were not made after once establishing the pressure loss for a particular vane size. The SSME ducts used for testing had no pressure sensing ports so no ΔP was measured. The input to the test meter had no flow

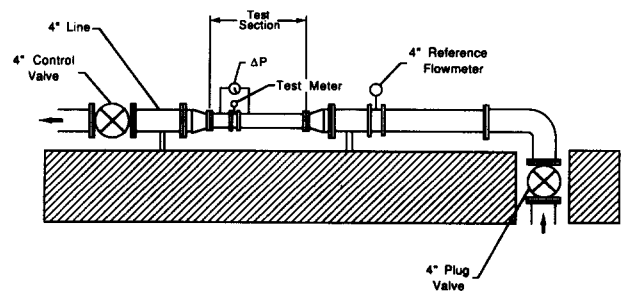

Figure 1 The water flow test facility. The test section can be either straight or an SSME duct

conditioning other than the 20 diameters of straight duct upstream. The reference meter was located directly upstream of the test section. The vortex shedding frequency of the reference and test meters differed by a factor of about 10 which should have eliminated any interference at the test meter. No interference was apparent.

Liquid nitrogen (LN_2) flow tests were carried out on the cryogenic flow test stand at NASA/Marshall. This system could hold constant pressures at the flowmeter. The LN_2 source for these tests was a large spherical tank which could be pressurized to more than 20 MPa (3000 psi). The LN_2 discharged through the test section, through a reference flowmeter consisting of a 4-inch water calibrated turbine meter, through a back pressure control valve, and then to a vent. Only one flowmeter has undergone cryogenic flow testing thus far.

In more recent tests, a fast Fourier transform (FFT) spectrum analyzer measured the frequency from the reference meter and the test meter. At the same time, narrow band signal spectra from 0 frequency to less than $2f$, where f is the vortex line frequency, were recorded as well as spectra from 0 to 10 kHz.

At the beginning of the project counters were used to count the vortex shedding frequency. A charge amplifier followed by a band pass filter was required to condition the output signal of the test meter for the counter. An older model spectrum analyzer was used to qualitatively view the signal.

The pressure loss across the meter was measured with a 0.7 MPa (100 psi) range transducer whose zero could be adjusted at the downstream side operating pressure to remove base pressure induced zero shifts of the transducer.

The LN_2 supply for testing was limited so signals from short periods of flow at each set point were amplified and tape recorded. The output signal was analyzed from the tapes later using the spectrum analyzer. The water flow tests were analyzed directly since flow time was not limited.

Two of the SSME ducts provided to NBS for meter testing are illustrated in part in Figures 2(a) and 2(b). These ducts have multiple out-of-plane bends, a geometry known to generate swirl. A $1\frac{1}{2}$-inch and $2\frac{1}{2}$-inch straight bladed turbine meter were used to measure the average axial swirl component in some water tests.

Vortex sensing

The extreme environment in which the meter is to be used and the design constraints imposed by the shuttle ducts mean that not only the vane shape, but also the vane suspension and a vortex sensing element had to be developed. The suspension and sensor design is still an ongoing project, partially because of the different duct sizes, but also because of some shortcoming of the designs used successfully thus far. Some of the vortex sensing designs tested are described below.

The vortices from the first vanes tested were sensed via a pressure port on one side of the vane that connected to an external transducer referenced to atmospheric pressure. Commercial meters with pressure sensors measure ΔP instead. From these tests it became immediately clear that such a detector would not suffice for vanes of small cross section. The signal was noisy and the porting seriously weakened the vane mechanically. Vanes fractured after a short period at the highest flows.

Another meter design consisted of a single piece vane and mount. The mount on the sensor end was a flat spring section immediately external to the duct wall. A strain gage on the spring served as the vortex sensor. The shedding vortices produced a time varying lift on this vane. The strain gage measured this lift and produced a periodic signal with a high

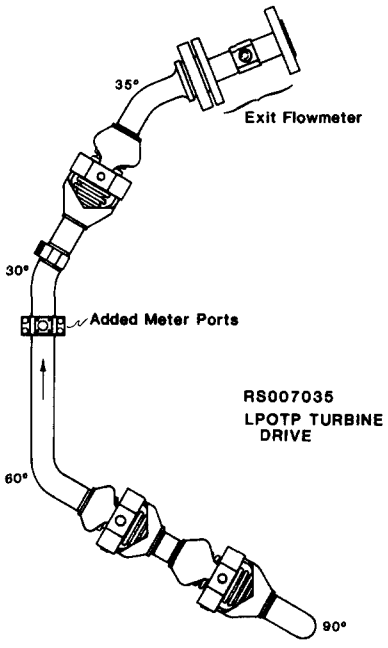

Figure 2(a) Scale drawing of the exit half of low pressure oxygen turbo pump drive duct, RS007035. A 90° bend and three 45° bends precede this section of the duct. The bend angles are shown

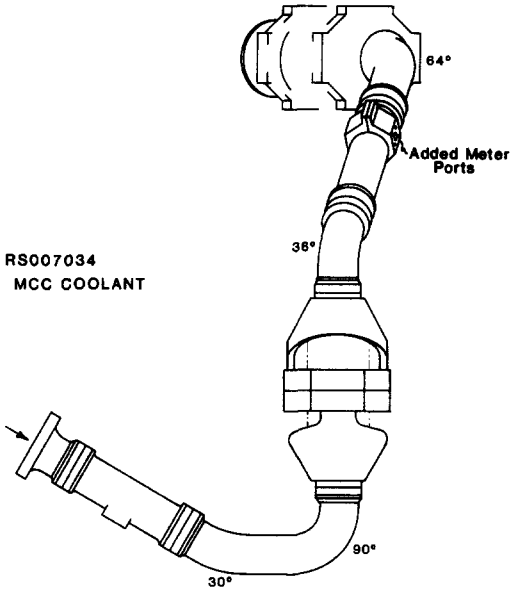

Figure 2(b) Scale drawing of the main combustion chamber coolant duct, RS007034. The duct bore is 50.8 mm

signal-to-noise (s/n) ratio. The s/n ratio was not quantitatively obtained.

This spring mount and strain gage sensor was unsuitable for LOX service because of the organic material in the strain gage and because the spring probably allowed the vane to strike the sides of the installation port at higher flows.

Yet another design consisted of a piezoelectric ceramic disc. This electroded lead zirconium titanate (PZT) disc was pressed against a vane support via an O-ring sealed drive pin. The time varying forces acting on the disc caused it to produce a time-varying voltage. Several versions of meters using PZT sensors to sense the vortices were tried prior to the meter design shown in Figure 3. This was one of the first meters tested that was designed both for cryogenic temperature and high pressure. The vane mounting had also evolved. The vane shown in Figure 3 is supported by a bayonet fitting on one side of the duct. The opposite end of the vane is connected by a clevis pin to the clevised end of a post. The post is an integral part of the top flange plate.

The objective of the sensor design shown in Figure 3 is to permit the calibration of the meter in water for flow measurement in LOX should this prove feasible. This dictates that the PZT either be made waterproof or be external to the duct. The sensor consists of a PZT disc set between two diaphragms where it is at ambient pressure. The pressure load on the diaphragms is supported by the PZT in the center. A series of concentric close fitting rings support the remaining diaphragm area from the PZT out almost to the seal. The duct pressure accesses the diaphragm on the side opposite the sensor along the drive pin. The pressure on diaphragms on the sides away from the PZT sensor are equalized through an interconnecting tube. A sealed adjusting screw in the top cap preloads the PZT against the vane via the drive pin. The concentric rings allow some displacement of the sensor to adjust the preload while maintaining the diaphragm spacing.

Another version of a vane support used the same vortex sensor. The vane mounting post was much shorter and notched about half way through just above the clevis holding the vane. A drive pin parallel to the vane axis but offset as far as the port diameter allowed towards the open side of the notch extended up to a sensor like that in Figure 3. The notch and drive pin arrangement is shown in Figure 4 for a cantilevered vane. The sensor axis was coincident with the drive pin axis. The flex at the notch was sensed in this arrangement. The design shown in Figure 3 or a water test version of it with an O-ring seal on the drive pin instead of the diaphragms has been used in most tests.

The PZT sensor is subjected directly to the duct pressure in the design shown in Figure 3. Pressure fluctuations from flow noise have not obviously contributed to the background noise during water tests. The pressure in the SSME ducts is 10 to 15 times higher and delivered by pumps. Pressure noise could become a much larger component of the signal. Because of this, sensors not subject to pressure noise and without diaphragms are desired.

Two mechanical displacement detectors have been tested as

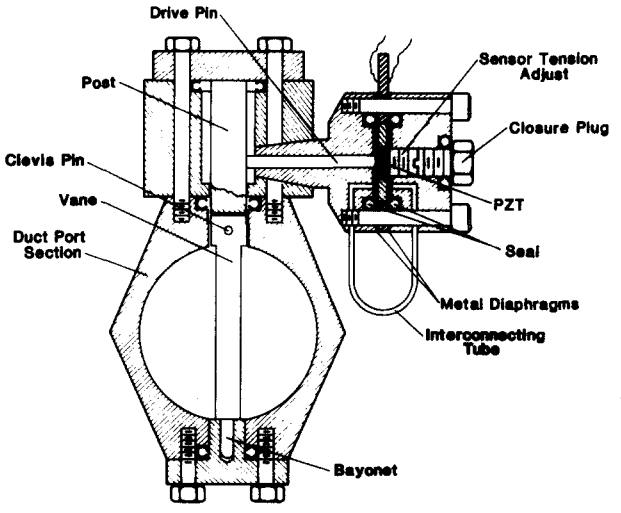

Figure 3 A scale drawing of a 59 mm bore meter for cryogenic service at high pressure

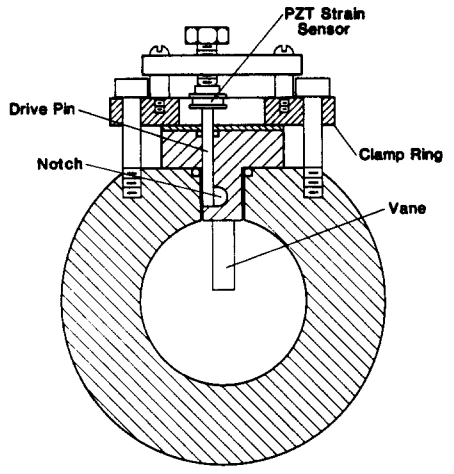

Figure 4 Cantilevered vane partially spanning the duct in a wafer type meter body

vortex sensors. The first consisted of an optical device which was tried during the LN_2 flow tests. The signal was lost in the noise at the recording instruments at lower flows. At the maximum flow, the spectrum line obtained was qualitatively the same as that obtained from the PZT sensor.

The second position detector was an eddy current coupled device. In some water tests the detector gave results similar to a PZT detector, except at the lowest flows where the s/n ratio decreased. None of the position sensors were configured to handle the pressure and temperature in the ducts. They are not LOX compatible since organic materials are used in their construction.

Only designs that did not require development of specialized fabrication techniques have been tried. Specialized techniques, such as potting the eddy current sensor coils in a glass or ceramic rather than epoxy may be necessary to produce a pressure-insensitive vortex detector for high pressure cryogenic use.

Experimental results

Well over a hundred different vanes were tested in the course of this work. Only a few can be discussed here. The vane cross-sectional shape, the vane length, suspension design, detector design, and meter body design were varied. Descriptions of the vanes discussed in this paper are found in the Appendix.

The vane shape, mounting, and the method of sensing vortices were investigated in parallel. The parallel development often precludes direct comparisons between the earlier and later test results. The earlier tests were not repeated because it did not serve the objective of the project to do so. The parameters examined to evaluate the performance of a meter design were the frequency width of the vortex line, the s/n ratio of this signal, and whether additional lines appear in the spectrum. The signal amplitude of VS flowmeters fluctuate randomly with time to varying degrees. The signal can fade completely for a few cycles of the shedding frequency. The number of cycles lost was generally proportional to flow so the flow dependence of the signal would not change, but the meter factor is altered. Some signal fade occurred for all the vanes tested. Qualitatively, the vanes with the least fade generally had the narrowest lines, the highest s/n ratio, and the lowest scatter. Often they had the best linearity and the meter factor was closest to constant over the flow range of interest. The narrower the spectrum line, the higher the s/n ratio, and the less the fade, the better the performance of a vane. Quantitative values, though measured for line width and s/n ratio, are not given since they can vary with suspension and sensor design.

Vortex shedding flowmeters for liquids are linear up to the 6 m/s maximum flows found in most conventional piping, thus, the upper limit of the meter is not discussed in most VS flowmeter papers. It seems to be accepted that the upper limit of the useful meter range occurs when the flow cavitates at the vane.[13] The pressure loss across the meter, ΔP, has the same dependence as flow through a pipe:

$$\Delta P \sim \rho V^2$$

where ρ is the density, and V the flow velocity. When cavitation occurs it is dictated by the liquid pressure, the velocity, and the fluid vapor pressure. The higher the upstream pressure, the higher V^2 can be before the pressure at some point behind the vane becomes less than the vapor pressure and cavitation occurs.

Even though the Reynolds number of LOX and LN_2 are nearly a factor of 10 higher than water at the same flow velocity, water tests should show whether the meter can measure LOX to the desired velocity. One purpose of these tests was to demonstrate that the meter could achieve the required flow velocity, so the meter factor data are shown as a function of velocity.

The Reynolds numbers can be obtained from the flow velocity in the 58.4 mm (2.3 inch) bore meters by multiplying the velocity by 3.9×10^4 s/m for water and 3.3×10^5 s/m for LN_2. For water flow in the 50.8 mm (2 inch) diameter duct this conversion to Reynolds number is 3.4×10^4 s/m. For water flow in the 41 mm (1.61 inch) bore duct the conversion factor is 2.8×10^4 s/m.

The meter factors are presented here as frequency per meter per second of average flow. This can be expressed as a Strouhal number by multiplying by the vane width in meters. The meter factor is influenced by the vane depth (the dimension along the axis of the pipe), the shape and even the angle of rotation of the vane about its axis. It is not clear that all the parameters affecting the Strouhal number are yet known.

At the beginning of the program a vortex shedding flowmeter in the 4-inch diameter main LOX duct was desired. The velocity there was estimated to be as large as 56 m/s. The tests to determine whether metering at this velocity was possible were carried out in the $1\frac{1}{2}$-inch test duct.

A $1\frac{1}{2}$-inch commercial vortex shedder was tested first. The results indicated that the meter could measure flow to about 35 m/s. The shuttle disc vortex sensor of this meter was destroyed by the much higher flows. The pressure loss across the meter and the transverse pressure generated by the vortex shedding increases as the square of the velocity. The vortex sensor was overdriven by about a factor of 30. The shuttle disc sensor was replaced with a differential pressure transducer external to the meter. The meter factor of the 12.7 mm wide by 17.2 mm depth vane was found to be 23.2 Hz·s/m. The pressure drop (ΔP) was proportional to the flow squared and extrapolated to about 3.7 MPa (540 psi) at 56 m/s flow, as the flowmeter manufacturer estimated.

The large ΔP was unacceptable. A reduction in the vane width to 6.4 mm and the depth to 9.5 mm succeeded in reducing the head loss by more than a factor of 4. Otherwise, ΔP remained proportional to velocity squared. Again the vortex-generated signal was poor but approximately constant with flow. The meter factor was 22.6 Hz·s/m, slightly less than that obtained for the commercial meter.

Figure 5 shows the meter factor obtained from a similar triangular vane with a 6.4 mm width. The X data were obtained with 20 diameters of straight pipe between the 4 to $1\frac{1}{2}$-inch converging section and the meter. The circles show the same

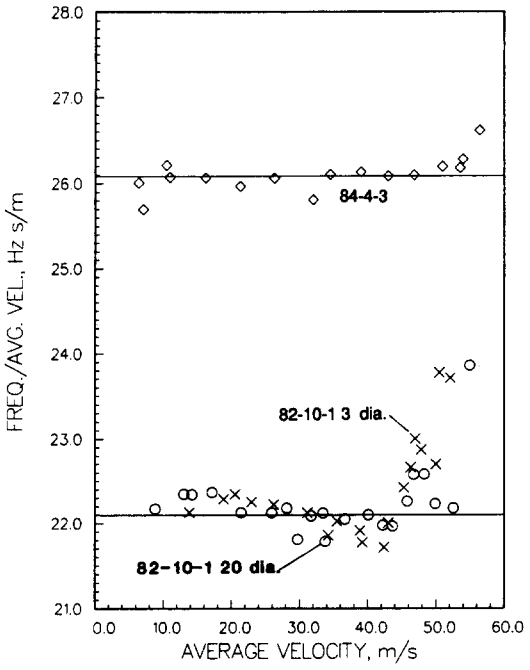

Figure 5 Meter factors of some vanes in the 41 mm bore straight test duct. Vane 82–10–1 was 3 diameters downstream, ×, and 20 diameters downstream, circles, of the 4 inch to 1–1/2 inch convergence section

meter about 3 diameters downstream from the converging section. The static pressure in the penstock was 5.4 MPa (790 psi). The vortex sensing was achieved through a pressure port in the vane. The data are approximately constant to 45 m/s flow for the downstream location and more than 53 m/s at the upstream location. A measurable vortex-generated signal remained to 56 m/s for the latter. This data is typical of all the test data obtained. A region of approximately constant meter factor changes to a flow dependent meter factor at high flows. The data scattered more in the flow dependent region. Above this flow dependent region the vortex signal vanished and the flow through the meter would not increase. In general, it was necessary to drop well under the maximum flow to reestablish the vortex signal. The increase of the meter factor and then the disappearance are assumed to be caused by cavitation at the vane. If cavitation does limit the maximum flow then changing the pressure changes the maximum flow. Figure 5 supports this assumption; the vane in the upstream location achieves a higher maximum flow. A meter that achieved 45 m/s maximum flow when tested on the 5.4 MPa section of the penstock only achieved a maximum flow of 36 m/s when only 3.9 MPa (570 psi) input pressure was available. The relationship between flow maximum and source pressure was not determined since the pressure at the meter was not measured. The horizontal lines in this and subsequent plots of meter factor versus flow are not fitted. They are provided for a reference to judge the constancy of the meter factor.

Rather than making the vane narrower to reduce the pressure loss, the blockage by the vane can be reduced as well by reducing the length. Such a vane is shown in Figure 4. Cousins and coworkers[9] have tested vanes with small gaps at the ends and found that the gaps strongly alter the meter performance. They assume flow along the vane axis causes the perturbation. A vane partially blocking the pipe should experience this flow. The flow velocity by the vane should vary along its length which must be detrimental to the vortex shedding process. In spite of this, it was found that vane 84–4–3 with a slightly trapezoidal cross section, 5.1 mm wide by 4.3 mm deep and 17.8 mm long in the 41 mm diameter pipe, had a nearly acceptable performance. The meter factor shown in Figure 5 for vane 84–4–3 was flat to 55 m/s even with the water supply from the penstock restricted because of the winter shut-down. The vortex spectrum lines obtained were 2 or 3 times wider and the s/n ratio was significantly poorer than obtained for a full length vane. More than two dozen variations of the vane design were tried to little avail in an attempt to improve the spectrum. These included a small disc (11.2 mm was the maximum diameter allowable) on the end of the vane as well as modifications of the nominally 5.1 by 4.3 mm cross section. Further work on the design stopped with the discovery that when the vane was scaled up linearly from a 41 mm (1.61 inch) duct size to 59 mm duct, the performance was degraded. No modification of the vane cross section or length improved the spectrum lines in the 59 mm (2.3 inch) diameter duct.

A decision not to install a VS meter in the 4-inch LOX duct coincided with the converting of the hydroplant at the test facility to remote operation. This displaced the test facility to a higher point on the penstock where the maximum pressure was 3.9 MPa (570 psi) precluding any additional testing to raise the maximum flow capacity of the meter at the 5.4 MPa (790 psi) source pressure.

The next highest LOX velocity occurs in the low pressure oxygen turbopump drive duct or 7035 duct shown in Figure 2(a). The maximum LOX velocity in this 58.4 mm diameter duct is a little under 30 m/s (98 ft/s). Tests of a meter for this duct were first done in the 59 mm diameter straight test section. The effect of varying the cross-sectional dimensions of some rectangular cross-sectioned vanes was investigated in this duct. Figure 6 shows the meter factor of three vanes as a function of flow velocity for w/D, where w is the vane width and D the pipe diameter, from 0.109 to 0.163 with d, the cross-sectional dimension parallel to the pipe axis, varied so d/w was constant at 2/3. In Figure 7, w/D was held constant at 0.13 while d/w

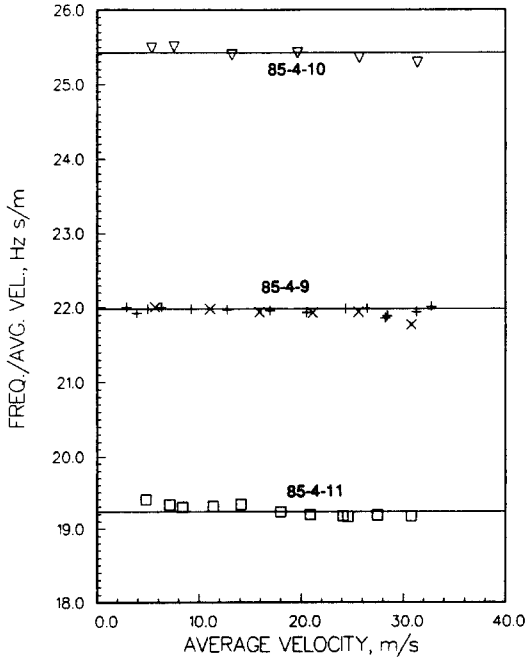

Figure 6 Meter factors of vanes with rectangular cross sections and varying values w/D in a 59 mm bore straight test duct. $d/w \cong 2/3$ for all three. 85–4–10, $w/D = 0.0109$; 85–4–9, $w/D = 0.129$; 85–4–11, $w/D = 0.163$

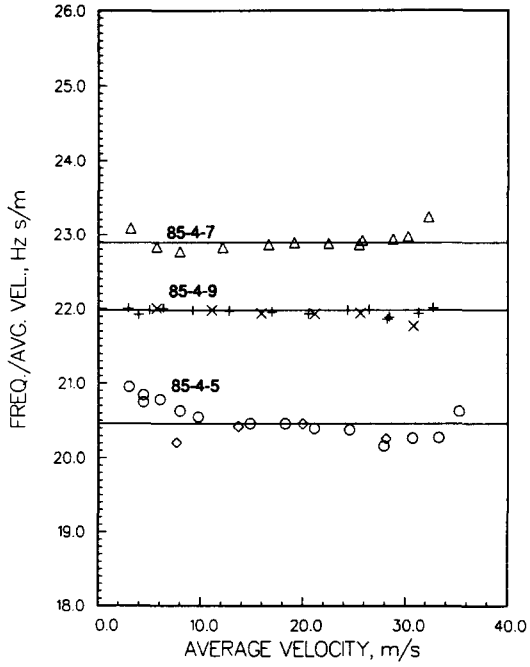

Figure 7 Meter factors of vanes with rectangular cross sections varying d/w in the straight test duct. $w/D=0.129$ for all three, 85–4–7, $d/w=0.55$; 85–4–9, $d/w=2/3$; 85–4–5, $d/w=0.86$

varied from 0.55 to 0.86. The center curve in both figures are the same vane and data. This vane, 85–4–9, qualitatively performed the best. The values of w/D and d/w are 0.13 and 2/3, respectively. The estimated pressure drop for LOX at maximum flow is about 34 kPa (50 psi).

Vanes of rectangular cross section with a $d/w=2/3$ are used in at least one brand of commercially available flowmeter though w/D is about twice as large. Vanes with cross-sectional shapes very similar to other commercial shapes, triangular such as 82–10–1 and 82–12–1 (see Appendix), T-shaped, and trapezoidal, were tried at various times through these tests. Some are described in the Appendix. Vanes 82–10–1 and 82–12–1 seemed to give good results until the instrumentation was improved. Then it became evident that vanes with rectangular cross sections gave better overall performances in terms of linearity and signal quality than the triangular, trapezoidal, and T-shapes tried. A T-shaped vane, 85–4–1, gave one of the highest s/n ratios, but was nonlinear. The vane, made of brass, also broke before the test was complete. Some additional and poorer performing T-shaped vanes were tried. Their fragility, the difficulty of machining accurate dimensions in such tiny sizes, and the generally better performance of the rectangular shape precluded trying more variations of the T-shape.

Because the rectangular shape was superior to other shapes tested, most of the vanes tested were rectangular. Not enough nonrectangular shapes were tested to assert that no superior cross-sectional shape exists for this application.

Some tests were done to determine how the sharpness of the leading corners of a rectangular vane affected the meter factor. As Figure 8 illustrates, rounded corners on vane 85–4–8 caused a 6% increase in meter factor. The beveled corners on 86–3–1 caused an increase of meter factor of 12% at high flows. These results are contrary to results reported for the vane widths used in commercial designs.[9] For those, rounded corners did not change the meter factor.

Variations of other parameters cause changes in performance. Recent tests have shown that the meter factor is also sensitive to the angle of rotation of the vane about its axis relative to the center line of the pipe. A 4° to 5° rotation was found to raise the meter factor by 10%. This disagrees with the test results of Cousins, Foster, and Johnson,[9] who found very little effect from rotating the vane even by 10°.

The cross-sectional dimensions of the vanes have been held to about 0.03 mm over the vane length. Whether tighter specifications would improve performance has yet to be established. Variation in the stiffness of the vane suspension did not affect the meter factor but some suggestion was found that a loose fit between the vane end and the clevis altered the meter factor slightly for vanes having a bayonet connection to the opposite side of the duct, as illustrated in Figure 3.

Vane 85–4–9 gave a constant meter factor and sharp spectra in the straight duct. This vane was tested in the 7035 duct. For the first tests the vane was placed in a short meter body at the exit of the duct as shown in Figure 2(a). A spectrum obtained with the vane axis parallel to the plane of the final bend is shown in Figure 9(b) and perpendicular to the plane of the bend is shown in Figure 9(a). The spectrum line is obviously much narrower for the latter configuration. Cousins also reported a better performance for the perpendicular orientation in his meter tests at lower flows.[9]

Vanes 85–4–7, 85–4–9, and 85–4–10 were tried in the exit meter with the vane axis perpendicular to the plane of the preceding bend. The meter factor of 85–4–9, in contrast to the straight duct results, now showed a definite flow dependence. Vane 85–4–7 was more linear with flow. A swirl measurement with a straight bladed turbine showed a $2\frac{1}{2}°$ average axial swirl at the duct exit. The swirl was obviously not uniform at this location. The turbine blades bent at the higher flows.

An opposed pair of instrument ports were silver soldered to the 7035 duct as shown in Figure 2(a) with the port axis perpendicular to the plane of the final three bends. They were located near the downstream end of a straight section preceded by a 60° bend. Vane 85–4–7 was tested in this location. Sharp spectrum lines were obtained. The meter factor is shown by the lower curve in Figure 10. The 7035 duct has a 90° bend

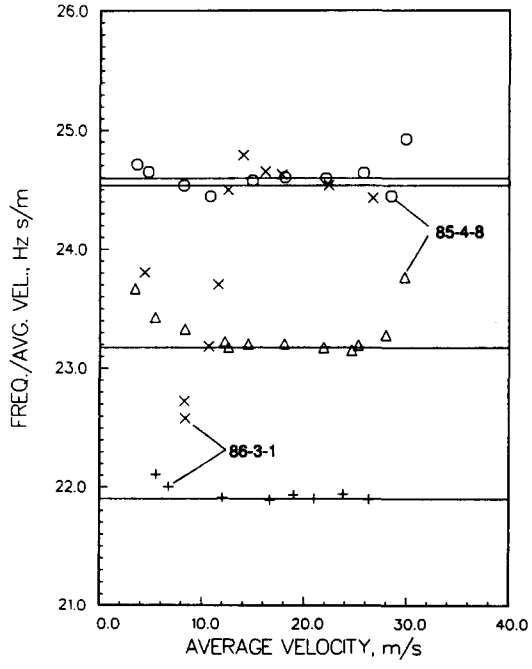

Figure 8 Effect of rounded and beveled corners on the meter factor. Triangles, 85–4–8 with sharp corners forward; circles 85–4–8 with rounded corners forward. Plus, 86–3–1 with sharp corners forward; ×, 86–3–1 with beveled corners forward

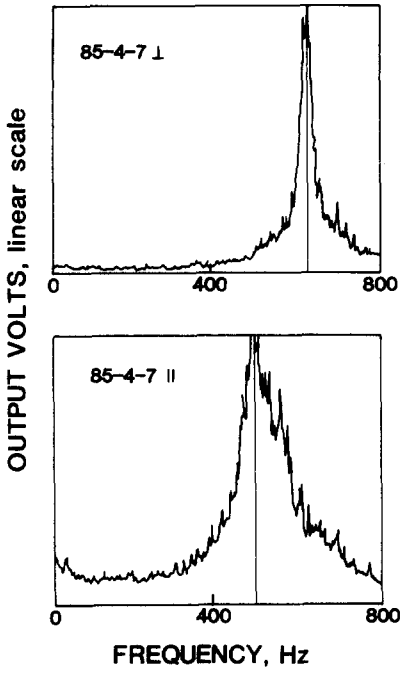

Figure 9 Signal spectrum lines from vane 85–4–9 in a meter at the exit end of the 7035 duct: (a) the vane axis perpendicular to the plane of the exit bend; (b) the vane axis parallel to the exit bend

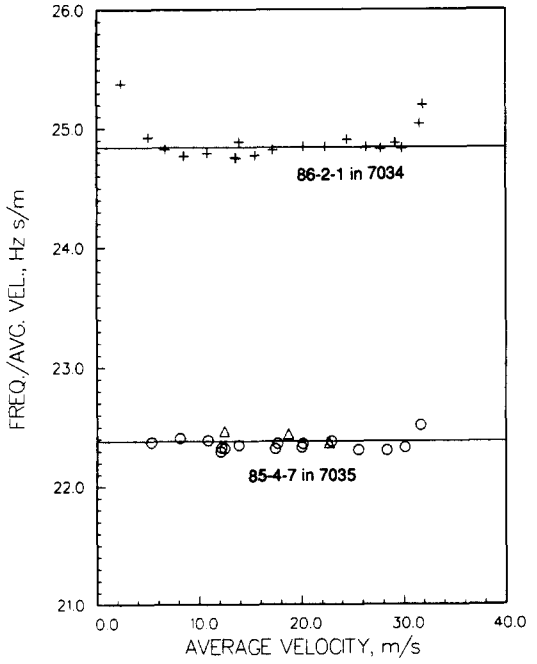

Figure 10 Meter factor of vane 85–4–7 in the 7035 duct in the ports preceding the 30° bend, lower line. The upper line is the meter factor of vane 86–2–1 in the 7034 duct

followed by three 45° bends then a 90° bend prior to the 60° bend. No two of these bends are in the same plane. The performance of 85–4–7 was not adversely affected by any flow distortion or swirl produced by the duct bends. A downward shift in the meter factor relative to the straight test duct occurred, however.

To test whether the combination of bends in the 7035 duct might be such that any swirl and flow distortions generated may be cancelled out at the meter site by a fortuitous combination of bends, a pair of ports was brazed to the 7034 duct at the location shown in Figure 2(b). The meter port axis was again perpendicular to the plane of the 36° bend immediately upstream. A 30° and a 90° bend precede the 36° bend. The plane of these two bends is 120° with respect to the plane of the 36° bend. Vane 86–2–1 was water flow tested in this duct. The vortex-generated spectrum lines were again narrow. The meter factor obtained is shown in Figure 10. The bends in this duct again did not adversely affect the meter performance.

Vanes placed in tension across the LOX duct were deemed undesirable for the SSME because of changes in duct diameter due to temperature and pressure changes. The bayonet mount shown in Figure 3 allows for differential motion between the duct and vane but sliding joints in the presence of LOX are also undesirable. The double cantilevered vane shown in Figure 11 was designed to affect a single piece vane without either coupling the sides of the duct or requiring any sliding contact. Cantilevered vanes of equal length and the same cross section are inserted into opposite ports. They nearly touch at the center of the duct. Vane 86–4–2 produced sharp spectrum lines in straight duct flow tests. The meter factor is illustrated in Figure 12. The magnitude of the meter factor was within 1% of being the same as that of a single piece vane with the same cross section. This vane was selected for the LN_2 flow tests in the 7035 duct. This vane was not water flow tested in the 7035 duct before the LN_2 tests because the duct had already been sent to NASA Marshall in preparation for the LN_2 tests.

Representative spectra from the LN_2 tests are shown in Figure 13. The spectra are plotted in two forms on each plot. The upper curve shows $\log V_s^2$ where V_s is the signal voltage. The scale on the vertical axis applies to this curve. An s/n ratio can be obtained from this curve. The lower curve shows the signal voltage. This better illustrates the signal line width. The line of greatest magnitude is the vortex line. The other lines and some of the noise were introduced by the test stand signal processing, transmission, and recording equipment used for the measurements. The linewidths obtained were similar to those of the straight duct water tests. Linewidths from the best meters were around 3% of the vortex frequency.

The meter factor for LN_2 is shown in Figure 12. The scatter was higher than the straight duct water data probably because the number of averages were lower, 10 instead of 50, and because the LN_2 flow often drifted over the course of the measurement. The high scatter of the two lowest flow points resulted from

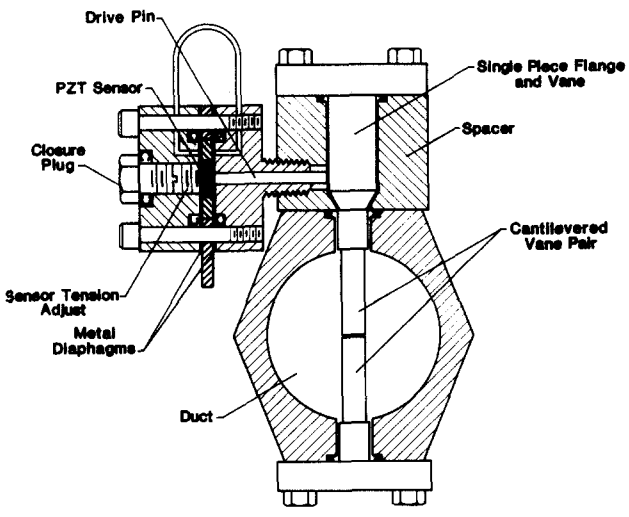

Figure 11 Diagram of the double cantilevered vane 86–4–2

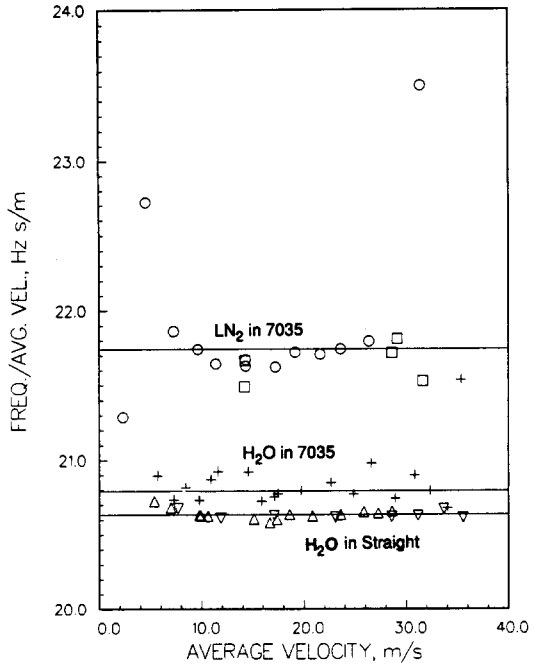

Figure 12 Meter factors for vane 86–4–2 in various ducts for water and LN_2. LN_2 in the 7035 duct circles are for a duct pressure of 2.5 MPa (360 psia) and squares are for a duct pressure of 3.5 MPa (510 psia). The pluses show the meter factor for water in the 7035 duct and the triangles show the meter factor for water in a straight duct

poor signal resolution. The LN_2 data also shows the effect of duct pressure on the linearity of the flowmeter. The meter factor at 32 m/s flow increased nearly 10% at the lower test pressure (circles). When the test pressure was raised the meter factor did not increase at 32 m/s (squares).

The 7035 duct was returned to Boulder after the LN_2 tests and vane 86–4–2 was water tested in this duct. The meter factor for this test is also shown in Figure 12. The meter factor was within 1% of the straight duct tests even though the spectrum lines were wide and often had multiple peaks. The vane actually performed better for LN_2 flow than for water flow in the 7035 duct.

A water calibrated turbine meter was used for the reference flowmeter on the NASA test stand. This meter was compared to the 4-inch reference meter at Boulder in the water flow facility and calibrated in liquid nitrogen at the LN_2 flow facility at the National Institute of Standards and Technology in Boulder. The meter factor for LN_2 was about 0.7% higher than for water. The meter factor of the 4-inch reference meter used at NBS was about $1\frac{1}{2}$% low assuming the more recently calibrated turbine meter was correct. With these adjustments applied, the LN_2 meter factor of 86–4–2 is still about $3\frac{1}{2}$% greater than the water meter factor. Small differences in the meter factor of a meter for LN_2 and water have been observed before. The difference seen here is larger but could easily be the result of biases in the calibration of the water and LN_2 test system reference meters. Shifts in meter factor between water and LN_2 flow of about 1.5% have been seen in other work for 2-inch and 4-inch meters.[14]

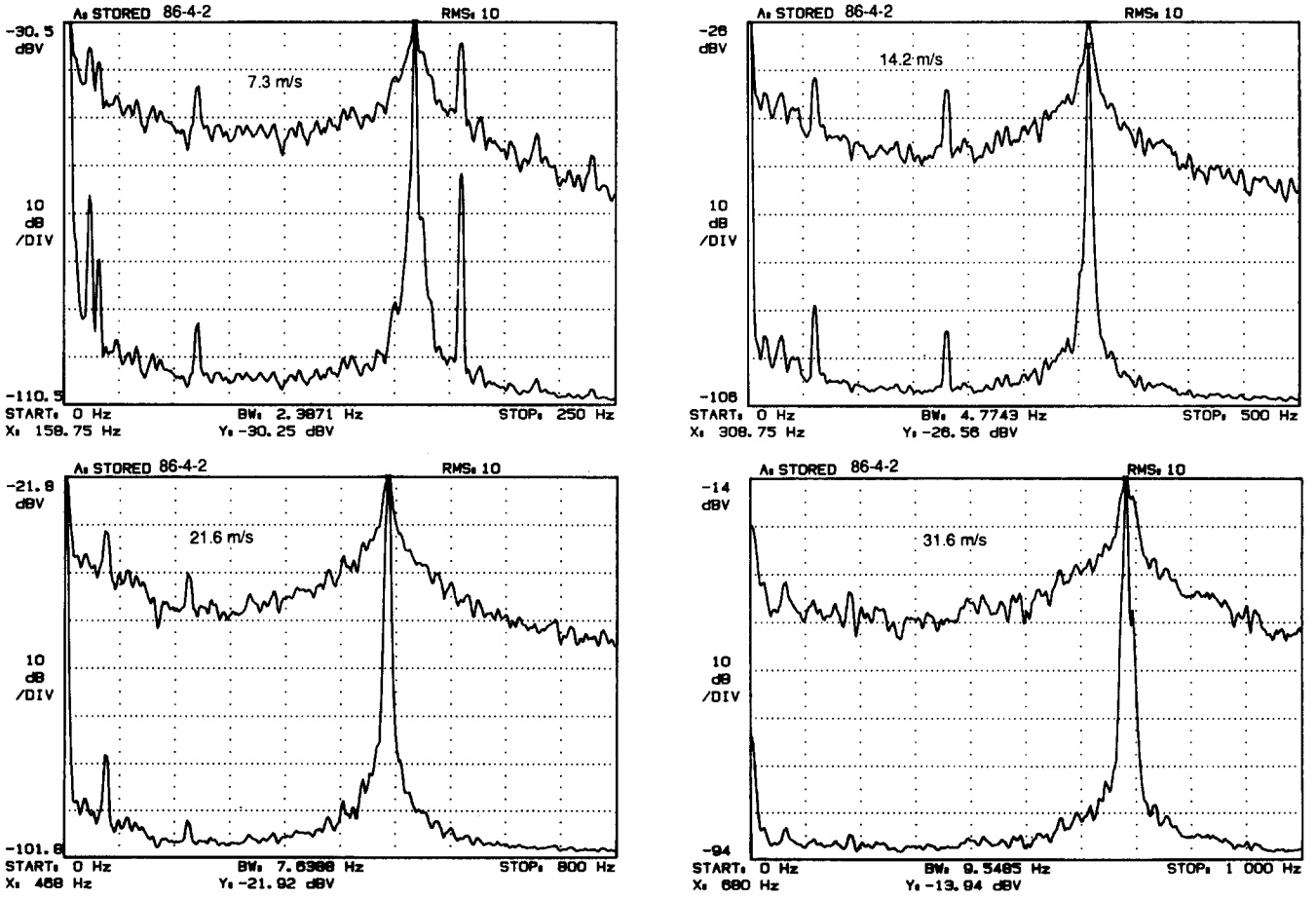

Figure 13 Narrow band width spectra for 86–4–2 from the LN_2 flow tests. Upper curve $\log(V_s)^2$ and lower curve, V_s. The secondary lines are introduced by the signal processing electronics and fade relative to the signal as flow increases

Table 1 Average meter factor of various vanes at high flows

Vane	Straight duct	Date	7035 duct	Date
86–4–2(#39)	20.63	4,5–86	20.8	7/87
85–12–1	20.	1–86	20.4	7/87
86–1–2	21.95	1–86	20.97	7/87
86–3–3	20.16	3–86	20.05	7/87
87–4–2	20.9	6–24–87	20.7	7/87
	20.8	5–27–87		
	20.8	5–15–87		
	20.9	5–11–87		
87–7–1	20.65	7–87	20.7	7/87
87–4–1	21.0	5–27–87		
	21.05	6–5–87		
	21.1	7–1–87		
85–4–7	23.1	2–7–86	22.24	8/87
	23.3	10–11–85	22.38	7/85
	23.2	3–6–86		
	23.1	3–6–86		

All vanes have rectangular cross sections. The d/w values are 0.85 except 86–1–2, $d/w=0.61$ and 85/4–7, $d/w=0.55$.

The water tests and the LN_2 tests at 2.5 MPa of 86–4–2 in the 7035 duct were carried to sufficiently high flow velocities that cavitation occurred. Even with the density difference between water and LN_2 and vapor pressure differences, the cavitation occurred in water and LN_2 at flows within ± 2 m/s of 30 m/s for similar pressures at the meter. The Reynolds numbers for water and LN_2 in the 7035 duct flowing 30 m/s is 1.2×10^6 and 1×10^7, respectively. The flow at which the meter cavitates is dictated primarily by the flow velocity as anticipated rather than by the Reynolds number.[13]

Table 1 shows meter factors obtained for a few of the many vanes tested. Repeated tests of a vane produced meter factors that differed by less than 1%. Thus, both the reference meter and the test meter factors remained stable. The meter factors agreed between the straight test duct and the 7035 duct within 1% for vanes with $d/w=0.84$ to 0.87 and $w/D=0.13$. The straight test duct for these tests consisted of a section of commercial steel pipe 25 diameters long with a rather uneven interior followed by a 4 pipe diameter long stainless steel meter section in which the meter ports were centered. The vortex spectrum lines obtained for all the 0.84 to 0.87 ratio vanes in the 7035 duct were usually broad and had multiple peaks. Narrow spectrum lines were obtained in the 7035 duct for both 86–1–2 and 85–4–7, $d/w=0.61$ and 0.55, respectively. The 7035 duct meter factors were about 4% lower than the straight duct meter factors for these two vanes.

Vanes with basically trapezoidal and triangular shapes, tried earlier in straight duct tests, were tried in the 7035 duct to determine if their meter factors might be less duct sensitive. None performed better than the vanes with rectangular shapes and most performed worse. Those with d/w values around 0.85 performed no better in the 7035 duct. Two vanes of nominally triangular shape with d/w around 0.81 gave better spectra but the meter factors differed between the two ducts by 5%. A shape which gives the same meter factor in the straight and 7035 ducts and produces narrow lines in the latter does not obviously exist.

Commercial VS meters, with the vanes dimensioned so that they operate at the minimum of the meter factor versus w/D curve, are much less sensitive to fluid properties than these meters with $w/d=0.13$. An increased fluid property dependence appears to be a phenomenon that must be tolerated when metering high flow rates.

The d value of the cantilevered pair could probably be decreased to provide a better vortex-generated spectrum line for water calibration in the 7035 duct. No evidence presently exists to suggest that such a vane would not behave as well in LN_2 flow and quite possibly even better than 86–4–2. However, continued testing of the double cantilevered vanes similar to 86–4–2 identified some undesirable features in that design. Many of the cantilevered pairs tested showed a meter factor as much as 4% larger than 86–4–2. This effect was tentatively ascribed to variations in vane stiffness until a series of tests with 87–4–1. These tests showed that the gap between the vane ends caused the larger meter factors. A gap of 0.6 mm causes a 4% increase in meter factor over that of a single piece vane. Though vane 87–4–1 was not very good in terms of performance, the test results shown in Figure 14 illustrate the sensitivity of the meter factor to the gap. It is not clear that this gap can be held either sufficiently small or fixed when the duct is cooled or at a high and varying pressure. A similar effect for a vortex meter was seen by Cousins *et al.*[9] for gaps between the end of the vane and the duct wall.

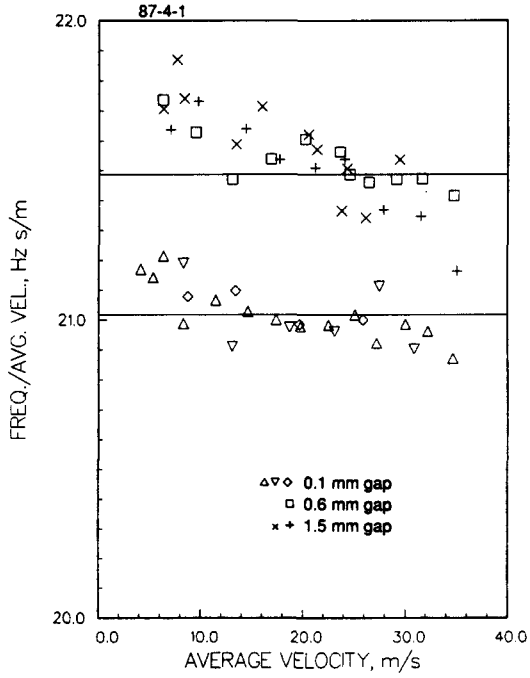

Figure 14 Meter factor of 87–4–1 in the straight 58.4 mm bore test duct showing the effect of the gap between the ends of the double cantilevered vane

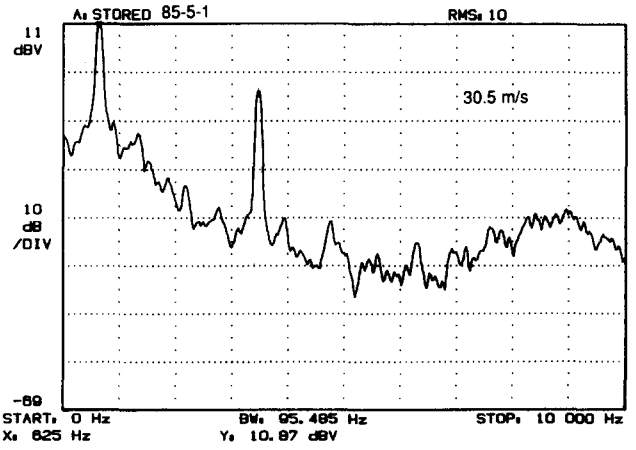

Figure 15 Wide band log V_s^2 spectrum of 87–5–1 illustrating the often present flow independent secondary lines

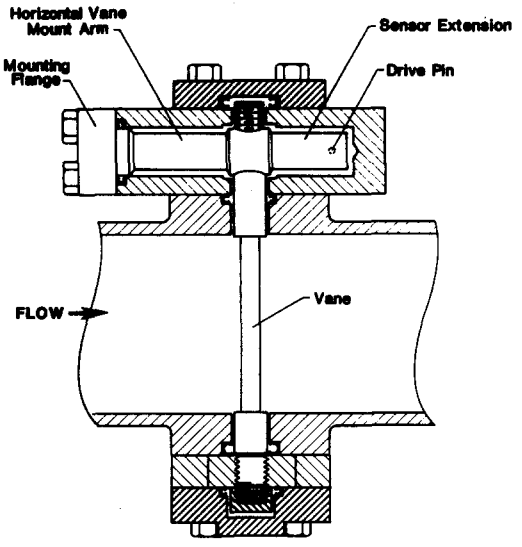

Figure 16 Side view of a vane suspension design providing axial strain relief

Another undesirable feature of the double cantilevered vane is illustrated by the spectrum in Figure 15 produced by vane 87–5–1 in the straight test section. The spectrum line of greatest magnitude is the vortex line but a strong flow independent line is present at 3.5 kHz. The performance of this vane was one of the best of the double cantilevered vanes. This line appeared only at the highest flows. Most other cantilevered pairs showed more and stronger secondary spectrum lines. Extra spectrum lines, especially those at frequencies near the vortex line, can complicate signal processing. A signal spectrum with only a clean, sharp vortex-generated line is preferred.

To retain the advantage of the single-piece vane the meter must be designed so the vane neither forms a rigid connection across the duct nor has a sliding connection. The high pressures in the duct are a significant impediment to realizing such a design.

Figure 16 illustrates a single piece vane that meets the above criteria. One end of the vane is threaded to the lower flange and secured by a locknut. The opposite end is clamped to a cantilevered arm mounted parallel to the duct. This arm is connected to a flange and contained in a hole in a block. This hole has a 3 mm greater diameter than the arm. This arm would be welded into the block for a cryogenic design. The arm can flex in the direction of the vane axis to relieve any stress produced by pipe dimension changes. Vortices produce transverse motion of the arm. This motion was detected by a sensor similar to that shown in Figure 3. The extension of the arm is not necessary but it does produce mechanical amplification of the transverse motion when used.

Vane 87–9–1 was constructed for this mounting and tested in the 7035 duct. The spectra obtained were among the best realized for any of these liquid meter designs. Some representative spectra are shown in Figure 17. The lines are narrow and the s/n ratio is high. No other lines than the vortex line appear in the 0 to 10 kHz band.

Comparison to other test results

A paper by Kalkhof[10] provides curves showing the Strouhal constant as a function of w/D for four values of d/w. Kalkhof notes that a d value for a nonrectangular vane can be obtained from $d = A/w$ where A is the cross-sectional area of the vane. Table 2 shows the Strouhal numbers for selected vanes from this work calculated from the meter factor times the vane width. These values are compared to the Strouhal numbers determined using w/D and d/w and the curves given in Kalkhof's paper.[10]

With the exception of vane 86–5–1, the agreement for

Table 2 Strouhal numbers from this work (meter factor x vane width) compared to those calculated using Kalkhof's results

Vane	A/w^2	*Triangular Vanes* w/D	S (this work)	S (Kalkhof)
41 mm bore, straight duct				
Commercial meter	1.01	0.310	0.295	0.275
82–9–1	1.10	0.156	0.141	0.161
82–11–1	1.10	0.156	0.147	0.161
7034 duct, 51 m bore				
87–9–2	0.82	0.125	0.150	0.162
		Rectangular Vanes		
Vane	d/w	w/D	S (this work)	S (Kalkhof)
41 mm bore straight duct				
83–6–2	0.8	0.125	0.161	0.158
85–5–1	0.67	0.125	0.175	0.164
7034 duct, 51 mm bore				
86–4–1	0.767	0.126	0.159	0.157
87–11–3	0.80	0.125	0.157	0.156
59 mm bore straight duct				
85–4–5	0.855	0.129	0.155*	0.155
85–4–7	0.55	0.129	0.174	0.170
85–4–9	0.67	0.129	0.167*	0.165
85–4–10	0.67	0.106	0.158	0.156
85–4–11	0.67	0.161	0.182	0.182
7035 duct, 58.4 mm bore				
85–4–7	0.55	0.130	0.170	0.170
87–9–1	0.55	0.130	0.166 to 0.169	0.170

* Average over test range.

rectangular vanes is close whether in the straight or SSME test ducts. Considering that rather large uncertainties must exist in determining the Strouhal numbers, the differences are probably indistinguishable. Sizable uncertainties are probably generated in the extrapolation of Kalkhof's curves to the w/d values of these vanes. Kalkhof's curves themselves are generated from four data points which often do not lie on the curves. The uncertainty of the test meter calibration factor, the vane dimensions, and using an average value for a nonlinear meter factor contribute additional uncertainties. These uncertainties combined are estimated to be larger than the differences between the Strouhal numbers obtained from flow and from the vane dimensions.

The Strouhal number for 86–5–1 was high. The corners of the vane were somewhat rounded which could easily cause an increase in the meter factor sufficient to give the increase in the Strouhal number.

The difference between Kalkhof's results and the smaller triangular vanes tested in this work are rather large. A large disagreement also exists between Kalkhof's and this work for the commercial vane.

For all rectangular vanes except 87–9–1, the Strouhal number

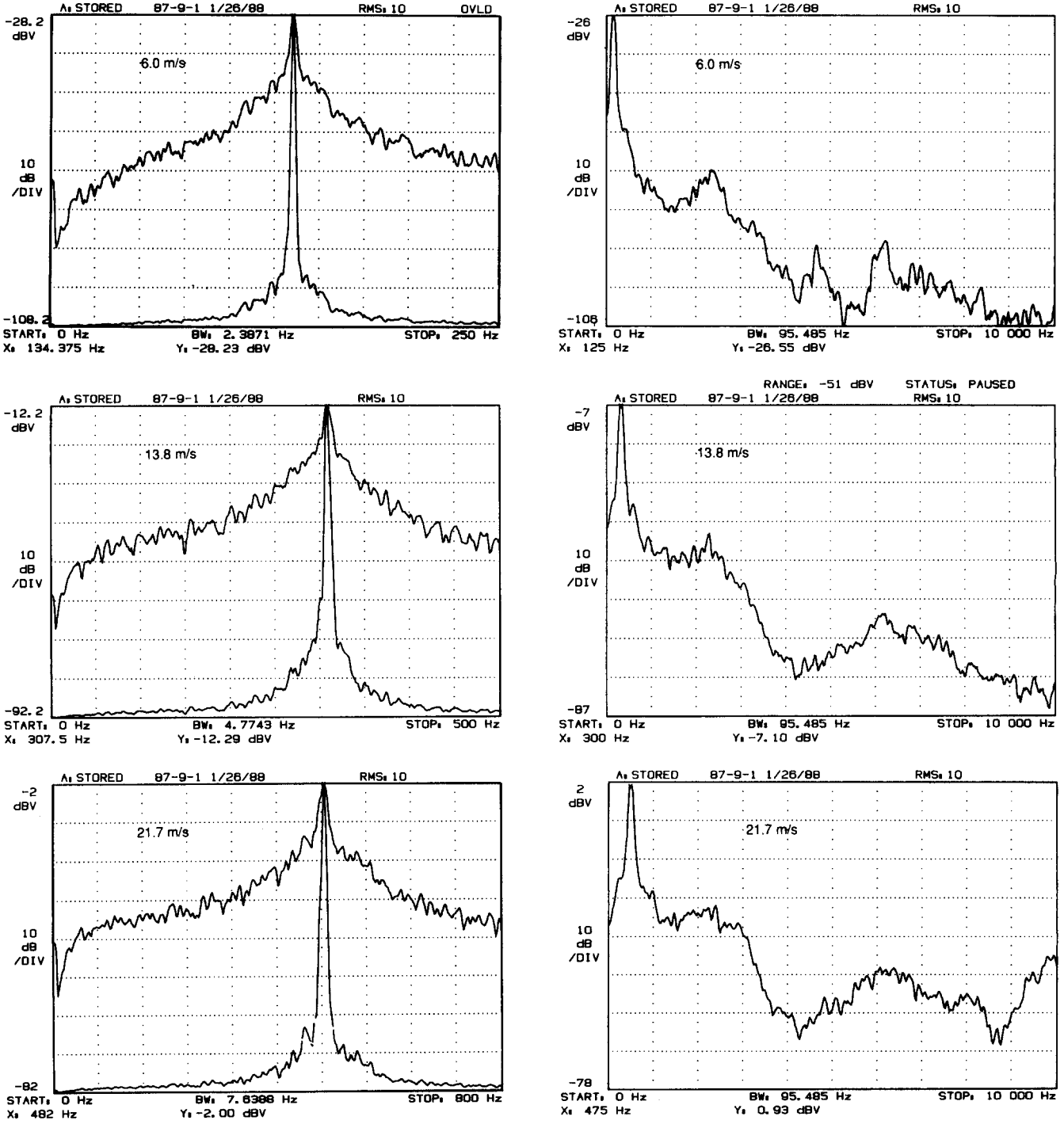

Figure 17 Some spectra from water tests of vane 87–9–1. Narrow band log V_s^2 spectra with the linear plot superimposed are shown on the left. The corresponding wide band spectrum is shown on the right

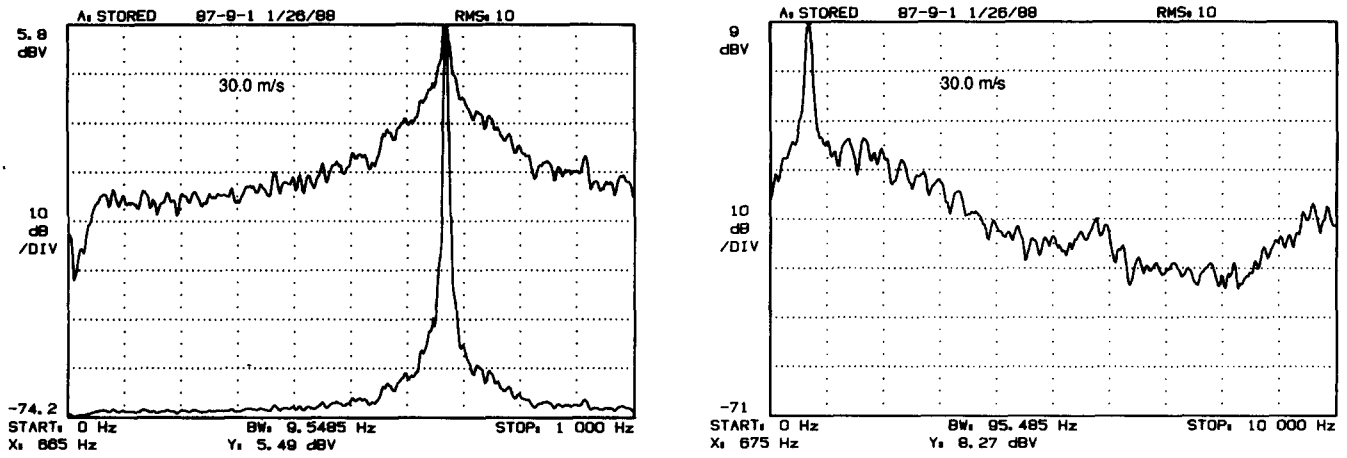

Figure 17 (continued)

calculated from the meter factor measurements exceeds those from Kalkhof's curves.[10] For the triangular vanes other than the commercial meter, the lower Strouhal numbers were calculated from the meter factor. This suggests the need for a weighting factor when calculating d from A/w.

The Strouhal numbers from this work do not agree as well with the rectangular vane results of Cousins *et al.*[9] as with Kalkhof.[10] Though the meter factors for the three rectangular vanes with $d/w=0.67$ increase with decreasing vane width as Cousins predicts, the ratio of the meter factor for $w/D=0.109$ to that for $w/D=0.16$ is an estimated 1.2 from Cousins work and 1.32 from this work. From Kalkhof's work[10] this ratio is an estimated 1.31. The reason for the difference is not known. Perhaps this difference results from the different test fluids, air from Cousins' work, and water for this and Kalkhof's work. Also, the duct sizes differ. Kalkhof used 4-inch ducts and Cousins used 6-inch ducts. Measurements to determine why this difference exists are currently outside the scope of the project.

Conclusions

Some vortex shedding flowmeter designs were tested at high flow velocities in a water and a liquid nitrogen flow test facility. The following conclusions can be drawn from the results obtained for vanes consisting of a uniform cylinder spanning the pipe:

(1) A vane in a 41 mm duct with a width 1/8 the pipe diameter can measure water flow at velocities up to 55 m/s (180 ft/s) with a maximum pressure loss less than 0.7 MPa (100 psi). This loss is proportional to the flow velocity squared. This result should apply as well to larger size ducts.

(2) Water and LN_2 flow tests show that an SSME duct can be metered through a diametrically opposite pair of the standard 11.2 mm diameter SSME instrument ports.

(3) The vanes mounted in the SSME straight sections as short as six diameters in length can give sharp signal spectrum lines and a linear response without any upstream flow conditioning. The vane should be mounted with its axis perpendicular to the plane of the preceding bend.

(4) A vane with a rectangular cross section and $0.67 \leq d/w \leq 0.85$ seemed to give the best results for water flow in terms of linearity, signal fade, and s/n power ratio in straight ducts, but vanes with $d/w \leq 0.6$ gave better results in the SSME ducts.

(5) Limited tests in flowing LN_2 have shown that the meter performs better for LN_2 than for water in the same velocity range. The Reynolds number in LN_2 is much higher than water at the same velocity.

(6) The Strouhal numbers obtained for these vanes agreed with the earlier work of Kalkhof[10] for vanes of rectangular shape. Vanes with rectangular shapes were the most successful. Vanes whose width decreased behind the front face, which are common in conventional VS meters, performed worse at high flows than the rectangular vanes.

(7) These results show that until more experience with these meters is obtained the vanes should be calibrated in the actual duct and with the actual fluid. With more test experience, this requirement might be relaxed.

Acknowledgments

The author wishes to thank the City of Boulder Water Utility for supplying the high pressure water used for these tests. The author also wishes to thank W. T. Powers and J. Ratley of the Instrumentation Group at NASA George C. Marshall Space Flight Center for arranging the LN_2 flow tests and R. L. Thompson, F. Hanks, and the test group for carrying out the tests.

References

1 Siegwarth, J. D. Vortex shedding flowmeters for liquids at high flow velocities. NASA Conference Publication **2372** (1985), 639–653

2 Siegwarth, J. D. Vortex shedding flow meter performance at high flow velocities. National Bureau of Standards Technical Note No. 1302 (October 1986)

3 Siegwarth, J. D. Vortex shedding flowmeter for fluids at high flow velocities. NASA Conference Publication **2437** (1986), 139–153

4 Wiktorowicz, W. E. Flow measurement by vortex shedding meters. *Proceedings 57th School of Hydrocarbon Measurement*, Norman, OK, 1982, p. 618. Available from K. E. Starling, 202 West Boyd, Norman, OK 73019

5 Flora, C. and Matsuura, T. K. Vortex flowmetering. *Meas. and Control (GB)* 1982, **15**, 165

6 Inkley, F. A., Walden, D. C., and Scott, D. J. Flow characteristics of vortex shedding flowmeters. *Meas. and Control (GB)* 1980, **13**, 166

7 Campbell, R. J. New vortex flowmeter uses ultrasonics. *Control Engineering* July 1973, 57

8 Prandtl, L. *Essentials of Fluid Dynamics*. Hafner, New York, 1952, 183 ff

9 Cousins, T., Foster, S. A., and Johnson, P. A. A linear and accurate flowmeter using vortex shedding. *Symposium of Power*

Fluids for Process Control, University of Surrey, Guildford, England, 1973, 45–56

10 Kalkhof, H. G. Influence of the bluff body shape on the measurement characteristics of vortex flowmeters. *International Conference on the Metering of Petroleum and its Products*, London Press Centre, London ED4, 1985

11 Corpron, G. P., Mattar, W. M., Richardson, D. A., and Sgourakes, G. E. Fluctuating pressure profile and sensor design for a vortex flowmeter. *ASME Annual Winter Meeting* (San Francisco, CA Dec., 15–18, 1978), American Society of Mechanical Engineers, New York, 1979

12 Pankanin, U. The influence of bluff body shape on the vortex signal quality. *International Conference on Flow Measurement in the Mid 80's*, National Engineering Laboratory, East Kilbride, Scotland, UK, June 6–12, 1986

13 Zanker, K. J. and Cousins, T. The performance and design of vortex meters. *Conference of Fluid Flow Measurements in the Mid 1970's*, National Engineering Laboratory, East Kilbride, Glasgow, 1975

14 Brennan, J. A., LaBrecque, J. F., and Kneebone, C. H. Progress report on cryogenic flowmetering at the National Bureau of Standards. *Instrumentation in Industry, Proceedings of the First Biennial Symposium* (Houston, Texas, October 11–14, 1976), Vol. 1, ISA, Pittsburgh, 1976

Appendix

The cross sections of most of the vanes tested can be described by the dimensions shown in Figure A1. Table A1 gives a description and the cross-sectional dimensions of those vanes discussed in this paper. The shape column refers to Figure A1. The letters following the duct size indicate the mounting:

P the vane is threaded on each end and bolted in. A pressure sensor detected the vortices.

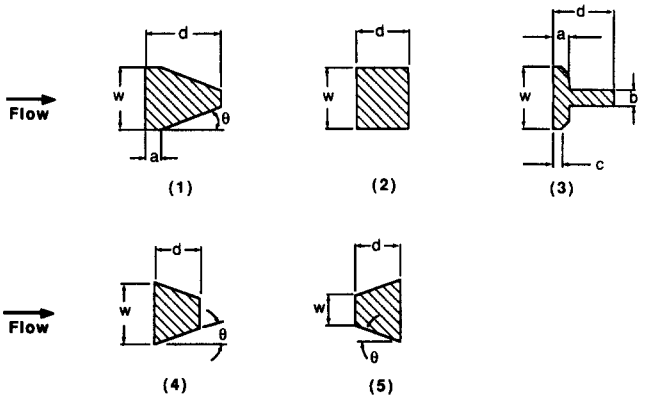

Figure A1

L These link vanes were connected to a clevis on each end and held in tension.

C These vanes were cantilevered from one side of the duct and only partially spanned it. See Figure 5.

B These vanes were attached by a clevis at the sensor end and were attached on the opposite end by a bayonet inserted into a spring loaded socket on the opposite end. See Figure 3.

DC These vanes cantilevered in from the opposite ports and nearly touched at the duct center. They were supposed to act like a single piece vane spanning the duct. See Figure 11.

HA These vanes were threaded into the flange on the fixed end. On the sensor end, they were secured to a horizontal arm with a nut. See Figure 16.

Table A1

Meter ID	Duct size (mm) and mounting	Shape	m (mm)	a (mm)	Remarks
1½" comm meter	41 P	1	12.7	17.2	$\theta=19°$
82-9-1	41 P	1	6.4	9.5	$\theta=17°$
82-10-1	41 P	1	6.4	9.5	$\theta=17°$
82-12-1	41 P	1	6.4	9.5	$\theta=17°$
86-3-2	41 L	2	6.1	6.1	
84-4-3	41 C	5	5.1	4.3	$\theta=2°$ length 17.8 mm
85-4-1	41 L	3	5.1	7.6	$a=1.7$ mm, $b=2.0$ mm, $c=0.3$ mm
85-4-5	59 L	2	7.6	6.6	
85-4-7	59 L	2	7.6	4.2	
85-4-8	59 L	2	7.6	4.2	Corners rounded ~0.4 mm radius
85-4-9	59 L	2	7.6	5.1	
85-4-10	59 L	2	6.2	4.3	
85-4-11	59 L	2	9.5	6.4	
85-5-1	41 L	2	5.1	3.4	
85-2-1	59 B	2	7.5	6.5	
86-1-2	59 B	2	7.6	4.6	
86-2-1	51 B	2	6.4	4.9	
86-3-1	59 B	2	7.6	5.1	Corners beveled 45° to 0.5 mm
86-3-3	59 B	2	7.6	6.4	Grooves down sides 0.5 mm behind face
86-4-2	59 DC	2	7.5	6.5	
87-4-1	59 DC	2	7.5	6.4	
87-4-2	59 DC	2	7.5	6.4	
87-5-1	59 DC	2	7.5	6.4	
87-7-1	59 DC	2	7.5	6.4	
87-9-1	59 HA	2	7.6	4.1	$\theta=3°$
87-9-2	51 HA	1	6.4	8.0	$\theta=20°$, $a=1$ mm